Int. J. Heat Mass Transfer. Vol. 32, No. 7, pp. 1239–1246, 1989
Printed in Great Britain

0017-9310/89 $3.00+0.00
Maxwell Pergamon Macmillan plc

Natural convection near a rectangular corner formed by two vertical flat plates with uniform surface heat flux

MAN HOE KIM
Department of Mechanical Engineering, Korea Advanced Institute of Science and Technology, P.O. Box 150, Cheongryang, Seoul, Korea

and

MOON-UHN KIM
Department of Applied Mathematics, Korea Advanced Institute of Science and Technology, P.O. Box 150, Cheongryang, Seoul, Korea

(*Received* 7 *November* 1988)

Abstract—The laminar natural convection flow along a rectangular corner formed by the intersection of two vertical quarter-infinite flat plates with uniform surface heat flux is considered. For large Grashof numbers, the leading-order corner-layer equations which govern the behaviour of laminar natural convection flow near the corner are derived and the appropriate boundary conditions are determined by using the method of matched asymptotic expansions. Solutions of the equations are numerically obtained for Prandtl numbers of 0.733 and 6.7. The general flow patterns and temperature distributions are similar to those with uniform wall temperature conditions except temperature profiles near the corner.

1. INTRODUCTION

A CONSIDERABLE amount of work has been devoted to the study of various aspects of natural convection boundary layers around a single heated plate, e.g. higher-order boundary layer effects around a vertical plate with uniform surface temperature [1, 2] or uniform heat flux [3], horizontal- and inclined-plate situations [4–6], and transient behaviour [7]. On the other hand, the natural convection near a corner formed by two planes has received little attention, in spite of its importance from theoretical and practical points of view.

Two-dimensional natural convection in a corner delimited by a vertical heated semi-infinite plate and a second plate forming an arbitrary angle has been considered by Luichini [8]. Liu and Guerra [9] studied theoretically the natural convection along a concave vertical corner submerged in a saturated porous medium. Reference [10] analysed the three-dimensional natural convection along a vertical rectangular corner formed by two quarter-infinite isothermal planes, and obtained velocity and temperature distributions for large Grashof numbers.

All of the above studies on the natural convection near a corner are for the cases that temperature distributions are specified on the surfaces. In practical applications as well as in many natural circumstances, however, the uniform heat flux condition on the surfaces is frequently met with. In this paper, we analyse the high Grashof number natural convection flow along a vertical rectangular corner formed by two quarter-infinite planes on which the uniform heat flux condition is imposed. Matched asymptotic expansions are used to derive the leading order corner-layer equations and the appropriate boundary conditions, in a similar way to that of refs. [10, 11]. Numerical solutions are obtained for both air ($Pr = 0.733$) and water ($Pr = 6.7$).

2. ANALYSIS

We consider the laminar natural convection flow along a corner formed by the intersection of two vertical quarter-infinite perpendicular flat plates dissipating heat uniformly. The present problem is formulated in a Cartesian coordinate system (x, y, z) with the origin at the starting point of the intersection. The x-axis coincides with the vertically upward intersection. Both y- and z-axes lie along the leading edges of quarter-infinite planes, respectively (Fig. 1(a)). Due to the geometrical singularity at the corner, the flow field and temperature distributions are inherently three-dimensional. The various regions delineated in Fig. 1(b) are designated as a potential flow (Region I), two boundary layers on plates $y = 0$ and $z = 0$ (Regions II and III), and a corner layer (Region IV), where the gradients in both the y- and z-directions are large compared to that in the x-direction.

2.1. *Corner-layer equations*

Employing the Boussinesq approximation and neglecting viscous dissipation, the governing equations are

NOMENCLATURE

a	grid spacing parameter, 0.2
Gr^*	modified Grashof number, $g\beta q_w x^4/kv^2$
H	mesh size, 0.02
k	thermal conductivity of fluid
L	arbitrary characteristic length
N, S	transformed independent variables
Nu	local Nusselt number
p^*	pressure in x, y, z coordinate system
p	pressure in ξ, η, ζ coordinate system
Pr	Prandtl number, v/α
q_w	surface heat flux
T	temperature
T_w	wall temperature
T_∞	ambient temperature
u^*, v^*, w^*	velocity components in x, y, z directions
u, v, w	velocity components in ξ, η, ζ directions
U_c	convective velocity, $(v/x)(Gr^*/5)^{2/5}$
x, y, z	Cartesian coordinate system.

Greek symbols

α	thermal diffusivity
β	thermal expansion coefficient
γ	$\lim_{\eta\to\infty}[\eta f_0'(\eta) - 4f_0(\eta)]$
θ	dimensionless temperature
μ	dynamic viscosity
ν	kinematic viscosity, μ/ρ
ξ, η, ζ	scaled independent variables
ρ	density of fluid
τ_w	wall shear stress
$\tau_{w\infty}$	wall shear stress as $\zeta \to \infty$
ϕ, φ	velocity potentials defined in equations (19)
Φ	velocity potential in potential region
ω	x-component of vorticity
Ω	modified vorticity function defined in equations (19).

$$\frac{\partial u^*}{\partial x} + \frac{\partial v^*}{\partial y} + \frac{\partial w^*}{\partial z} = 0 \tag{1a}$$

$$\frac{Du^*}{Dt} = -\frac{1}{\rho}\frac{\partial p^*}{\partial x} + \nu\nabla^{*2}u^* + g\beta(T - T_\infty) \tag{1b}$$

$$\frac{Dv^*}{Dt} = -\frac{1}{\rho}\frac{\partial p^*}{\partial y} + \nu\nabla^{*2}v^* \tag{1c}$$

$$\frac{Dw^*}{Dt} = -\frac{1}{\rho}\frac{\partial p^*}{\partial z} + \nu\nabla^{*2}w^* \tag{1d}$$

$$\frac{DT}{Dt} = \alpha\nabla^{*2}T \tag{1e}$$

where

$$\frac{D}{Dt} \equiv u^*\frac{\partial}{\partial x} + v^*\frac{\partial}{\partial y} + w^*\frac{\partial}{\partial z}$$

$$\nabla^{*2} \equiv \frac{\partial^2}{\partial x^2} + \frac{\partial^2}{\partial y^2} + \frac{\partial^2}{\partial z^2}.$$

Let us introduce the scaled dimensionless corner-layer variables as follows:

$$\eta = \frac{y}{x}\left(\frac{Gr^*}{5}\right)^{1/5}, \quad \zeta = \frac{z}{x}\left(\frac{Gr^*}{5}\right)^{1/5}$$

$$[u(\eta,\zeta), v(\eta,\zeta), w(\eta,\zeta)] = \left[\frac{u^*}{U_c}, \frac{v^*}{U_c}\left(\frac{Gr^*}{5}\right)^{1/5}, \frac{w^*}{U_c}\left(\frac{Gr^*}{5}\right)^{1/5}\right]$$

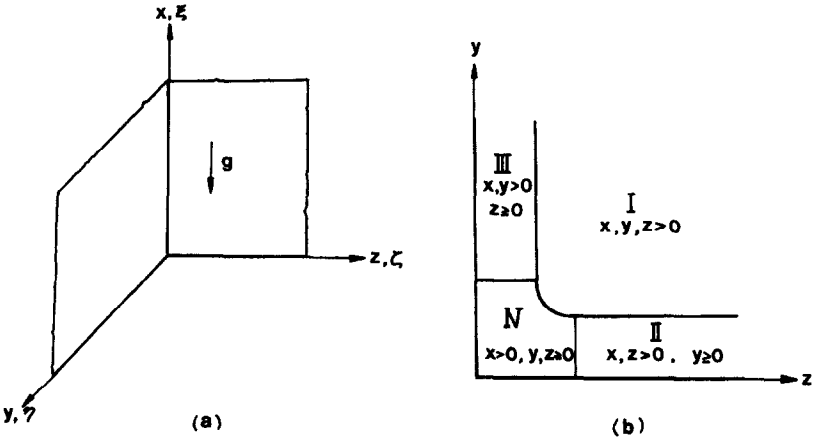

FIG. 1. Definition sketch: Region I, potential flow; Regions II and III, boundary layers; Region IV, corner layer.

$$p(\eta,\zeta)=\frac{p^*}{\rho U_c^2}\left(\frac{Gr^*}{5}\right)^{2/5}$$

$$\theta(\eta,\zeta)=\frac{k}{q_w x}(T-T_\infty)\left(\frac{Gr^*}{5}\right)^{1/5} \quad (2)$$

where η and ζ are the stretched similarity corner-layer variables; Gr^* and U_c denote, respectively, the modified Grashof number and the convective velocity

$$Gr^*=g\beta q_w x^4/kv^2$$

$$U_c=(v/x)\left(\frac{Gr^*}{5}\right)^{2/5}$$

In what follows, we assume that the modified Grashof number is sufficiently large such that $(Gr^*/5)^{-1/5}$ can be taken as a small perturbation parameter.

Substitution of equations (2) into equations (1) yields, to the leading order, the corner-layer equations, after eliminating the pressure terms in equations (1c) and (1d)

$$-\frac{1}{5}(\eta u_\eta+\zeta u_\zeta-3u)+v_\eta+w_\zeta=0 \quad (3a)$$

$$-\frac{u}{5}(\eta u_\eta+\zeta u_\zeta-3u)+vu_\eta+wu_\zeta=\nabla^2 u+5\theta \quad (3b)$$

$$-\frac{u}{5}(\eta\omega_\eta+\zeta\omega_\zeta+2\omega)+v\omega_\eta+w\omega_\zeta$$

$$+(v_\eta+w_\zeta)\omega+\frac{u_\zeta}{5}(\eta v_\eta+\zeta v_\zeta+v)$$

$$-\frac{u_\eta}{5}(\eta w_\eta+\zeta w_\zeta+w)=\nabla^2\omega \quad (3c)$$

$$\omega=w_\eta-v_\zeta \quad (3d)$$

$$-\frac{u}{5}(\eta\theta_\eta+\zeta\theta_\zeta-\theta)+v\theta_\eta+w\theta_\zeta=\frac{1}{Pr}\nabla^2\theta \quad (3e)$$

where

$$\nabla^2\equiv\frac{\partial^2}{\partial\eta^2}+\frac{\partial^2}{\partial\zeta^2}.$$

The set of non-linear equations (3) is to be solved throughout the region $0\leqslant\eta,\zeta\leqslant\infty$ with the boundary conditions which will be described in the subsequent subsection.

2.2. *Boundary conditions*

Note the following symmetry properties which are useful in describing the boundary conditions as well as the flow field:

$$u(\eta,\zeta)=u(\zeta,\eta),\quad v(\eta,\zeta)=w(\zeta,\eta),$$
$$\theta(\eta,\zeta)=\theta(\zeta,\eta)$$
$$\omega(\eta,\zeta)=-\omega(\zeta,\eta). \quad (4)$$

2.2.1. *Wall boundary conditions.* The conditions to be satisfied on the wall boundaries are the no-slip and uniform heat flux conditions

$$u=v=w=0,\quad \omega=w_\eta,\quad \theta_\eta=-1\quad \text{at}\ \eta=0$$

$$u=v=w=0,\quad \omega=-v_\zeta,\quad \theta_\zeta=-1\quad \text{at}\ \zeta=0. \quad (5)$$

2.2.2. *Far-field boundary conditions as* $\zeta\to\infty$, $\eta/\zeta\to 0$. The conditions at the far-field boundary for the corner layer ($\zeta\to\infty$) are given by the asymptotic matching with the solutions of the boundary layer (Region II) as $z\to 0$. Since the zeroth-order potential flow ($u=v=w=0$, $\theta=0$) does not satisfy the uniform heat flux condition $\theta_\eta=-1$ on the wall, the first-order boundary layer is introduced.

We assume the following series expansions for the boundary layer (Region II), in which x- and z-coordinates are unchanged, but the y-coordinate is stretched:

$$\bar{x}=\frac{x}{L},\quad \bar{Y}=\frac{y}{L}\left(\frac{\overline{Gr}^*}{5}\right)^{1/5},\quad \bar{z}=\frac{z}{L};$$

$$\frac{u^*}{\bar{U}_c}\sim\bar{u}_0+\bar{u}_1\left(\frac{\overline{Gr}^*}{5}\right)^{-1/5}+\cdots$$

$$\frac{v^*}{\bar{U}_c}\sim\bar{v}_1\left(\frac{\overline{Gr}^*}{5}\right)^{-1/5}+\bar{v}_2\left(\frac{\overline{Gr}^*}{5}\right)^{-2/5}+\cdots$$

$$\frac{w^*}{\bar{U}_c}\sim\bar{w}_1\left(\frac{\overline{Gr}^*}{5}\right)^{-1/5}+\bar{w}_2\left(\frac{\overline{Gr}^*}{5}\right)^{-2/5}+\cdots$$

$$\frac{p^*}{\rho\bar{U}_c^2}\sim\bar{p}_0+\bar{p}_1\left(\frac{\overline{Gr}^*}{5}\right)^{-1/5}+\bar{p}_2\left(\frac{\overline{Gr}^*}{5}\right)^{-2/5}+\cdots$$

$$\frac{k}{q_w L}(T-T_\infty)\sim\bar{\theta}_0\left(\frac{\overline{Gr}^*}{5}\right)^{-1/5}+\bar{\theta}_1\left(\frac{\overline{Gr}^*}{5}\right)^{-2/5}+\cdots \quad (6)$$

where $\overline{Gr}^*$ and $\bar{U}_c$ denote, respectively, the modified Grashof number and the convective velocity based on an arbitrary length L which should not appear in the final result

$$\overline{Gr}^*=g\beta q_w L^4/kv^2$$

$$\bar{U}_c=\frac{v}{L}\left(\frac{\overline{Gr}^*}{5}\right)^{2/5}$$

Substituting series (6) into equations (1), the first-order boundary layer equations are obtained as

$$\frac{\partial\bar{u}_0}{\partial\bar{x}}+\frac{\partial\bar{v}_1}{\partial\bar{Y}}=0$$

$$\bar{u}_0\frac{\partial\bar{u}_0}{\partial\bar{x}}+\bar{v}_1\frac{\partial\bar{u}_0}{\partial\bar{Y}}=\frac{\partial^2\bar{u}_0}{\partial\bar{Y}^2}+5\bar{\theta}_0$$

$$\bar{u}_0\frac{\partial\bar{\theta}_0}{\partial\bar{x}}+\bar{v}_1\frac{\partial\bar{\theta}_0}{\partial\bar{Y}}=\frac{1}{Pr}\frac{\partial^2\bar{\theta}_0}{\partial\bar{Y}^2};$$

$$\bar{u}_0=\bar{v}_1=0,\quad \frac{\partial\bar{\theta}_0}{\partial\bar{Y}}=-1\quad \text{at}\ \bar{Y}=0\ \text{and}\ \bar{u}_0\to 0,$$

$$\bar{\theta}_0\to 0\quad \text{as}\ \bar{Y}\to\infty. \quad (7)$$

Equations (7) have the solutions

$$\bar{U}_c\bar{u}_0 = 5U_c f_0'(\eta)$$

$$\bar{U}_c\left(\frac{\overline{Gr^*}}{5}\right)^{-1/5}\bar{v}_1 = U_c\left(\frac{Gr^*}{5}\right)^{-1/5}[\eta f_0'(\eta) - 4f_0(\eta)]$$

$$\frac{q_w L}{k}\left(\frac{\overline{Gr^*}}{5}\right)^{-1/5}\bar{\theta}_0 = \frac{q_w x}{k}\left(\frac{Gr^*}{5}\right)^{-1/5} t_0(\eta)$$

$$\eta = \frac{y}{x}\left(\frac{Gr^*}{5}\right)^{1/5} \tag{8}$$

where $f_0(\eta)$ and $t_0(\eta)$ are the solutions for two-dimensional natural convection on the vertical flat plate with uniform heat flux

$$f_0''' + 4f_0'' - 3(f_0')^2 + t_0 = 0$$

$$t_0'' + Pr(4f_0 t_0' - f_0' t_0) = 0$$

$$f_0(0) = f_0'(0) = t_0(\infty) = f_0'(\infty) = 0, \quad t_0'(0) = -1.$$

Solutions (8) imply that the corner-layer variables u, v and θ become asymptotically the corresponding two-dimensional values as $\zeta \to \infty$. The additional matching condition for the crossflow w is posed by considering the second-order boundary layer approximations in Region II. Observation of solutions (8) shows that the inflow velocity to the boundary layer which is absent in the zeroth-order potential flow appear

$$\bar{U}_c\left(\frac{\overline{Gr^*}}{5}\right)^{-1/5}\lim_{\eta\to\infty}\bar{v}_1(\eta) = \gamma U_c\left(\frac{Gr^*}{5}\right)^{-1/5} \quad \text{for } x > 0$$

$$\gamma = \lim_{\eta\to\infty}[\eta f_0'(\eta) - 4f_0(\eta)]. \tag{9}$$

This inflow velocity forces the introduction of the next-order potential flow. Since the flow field outside the boundary layers must remain irrotational, we define the velocity potential

$$(u^*, v^*, w^*) = (\Phi_x, \Phi_y, \Phi_z) = \bar{U}_c\left(\frac{\overline{Gr^*}}{5}\right)^{-1/5}(U_1, V_1, W_1).$$

With the matching condition on $y = 0$

$$\lim_{\eta\to\infty}\bar{v}_1 = \lim_{y\to 0} V_1$$

as well as the corresponding one on the opposite surface $z = 0$, we obtain the following boundary value problem for the first-order potential flow:

$$\frac{\partial^2\Phi}{\partial x^2} + \frac{\partial^2\Phi}{\partial y^2} + \frac{\partial^2\Phi}{\partial z^2} = 0$$

$$\Phi_y = \begin{cases} \gamma U_c\left(\dfrac{Gr^*}{5}\right)^{-1/5}, & \text{at } y = 0^+, x, z > 0 \\ 0, & \text{at } y = 0^+, x \leqslant 0, z > 0 \end{cases}$$

$$\Phi_z = \begin{cases} \gamma U_c\left(\dfrac{Gr^*}{5}\right)^{-1/5}, & \text{at } z = 0^+, x, y > 0 \\ 0, & \text{at } z = 0^+, x \leqslant 0, y > 0 \end{cases} \tag{10}$$

which can be solved directly with the use of a suitable Green's function. We find, after some calculations, that

$$\begin{aligned}
\bar{U}_c\left(\frac{\overline{Gr^*}}{5}\right)^{-1/5}U_1 = -\gamma U_c\left(\frac{Gr^*}{5}\right)^{-1/5}\Bigg[&\bar{\eta}^{-1}(1+\bar{\eta}^2)^{2/5} \\
&\times\left(\cos\frac{4}{5}\theta_1 + \cot\frac{\pi}{5}\sin\frac{4}{5}\theta_1\right) \\
&+\bar{\zeta}^{-1}(1+\bar{\zeta}^2)^{2/5}\left(\cos\frac{4}{5}\theta_2 + \cot\frac{\pi}{5}\sin\frac{4}{5}\theta_2\right) \\
&-\bar{\eta}^{-1}(1+\bar{\eta}^2)^{-1/10}\left(\cos\frac{\theta_1}{5} - \cot\frac{\pi}{5}\sin\frac{\theta_1}{5}\right) \\
&-\bar{\zeta}^{-1}(1+\bar{\zeta}^2)^{-1/10}\left(\cos\frac{\theta_2}{5} - \cot\frac{\pi}{5}\sin\frac{\theta_2}{5}\right)\Bigg]
\end{aligned}$$

$$\begin{aligned}
\bar{U}_c\left(\frac{\overline{Gr^*}}{5}\right)^{-1/5}V_1 = \gamma U_c\left(\frac{Gr^*}{5}\right)^{-1/5}&(1+\bar{\eta}^2)^{-1/10} \\
&\times\left(\cos\frac{\theta_1}{5} - \cot\frac{\pi}{5}\sin\frac{\theta_1}{5}\right)
\end{aligned}$$

$$\begin{aligned}
\bar{U}_c\left(\frac{\overline{Gr^*}}{5}\right)^{-1/5}W_1 = \gamma U_c\left(\frac{Gr^*}{5}\right)^{-1/5}&(1+\bar{\zeta}^2)^{-1/10} \\
&\times\left(\cos\frac{\theta_2}{5} - \cot\frac{\pi}{5}\sin\frac{\theta_2}{5}\right)
\end{aligned} \tag{11}$$

where

$$\bar{\eta} = y/x, \quad \bar{\zeta} = z/x$$

$$\theta_1 = \tan^{-1}\bar{\eta}, \quad \theta_2 = \tan^{-1}\bar{\zeta}.$$

The following asymptotic behaviours for the above solutions as $\bar{\eta}$ and $\bar{\zeta} \to 0$ are noted for the subsequent analysis:

$$\begin{aligned}
\bar{U}_c\left(\frac{\overline{Gr^*}}{5}\right)^{-1/5}U_1(x,y,z) \sim -2\gamma U_c\left(\frac{Gr^*}{5}\right)^{-1/5}&\\
\times\left(\cot\frac{\pi}{5} + \frac{1}{10}(\bar{\eta}+\bar{\zeta}) + \cdots\right)&
\end{aligned} \tag{12a}$$

$$\begin{aligned}
\bar{U}_c\left(\frac{\overline{Gr^*}}{5}\right)^{-1/5}V_1(x,y,z) \sim \gamma U_c\left(\frac{Gr^*}{5}\right)^{-1/5}&\\
\times\left(1 - \cot\frac{\pi}{5}\frac{\bar{\eta}}{5} - \frac{6}{50}\bar{\eta}^2 + \cdots\right)&
\end{aligned} \tag{12b}$$

$$\bar{U}_c\left(\frac{\overline{Gr}^*}{5}\right)^{-1/5} W_1(x,y,z) \sim \gamma U_c\left(\frac{Gr^*}{5}\right)^{-1/5} \times\left(1-\cot\frac{\pi}{5}\frac{\bar{\zeta}}{5}-\frac{6}{50}\bar{\zeta}^2+\cdots\right). \quad (12c)$$

The crossflow velocity W_1, which appears as a result of the mutual interaction of the boundary layers, leads to a second-order boundary layer flow.

Substituting boundary layer variables (6) into equations (1) and retaining the second-order terms, we have the following second-order boundary layer equations:

$$\frac{\partial\bar{u}_1}{\partial\bar{x}}+\frac{\partial\bar{v}_2}{\partial\bar{Y}}+\frac{\partial\bar{w}_1}{\partial\bar{z}}=0 \quad (13a)$$

$$\bar{u}_0\frac{\partial\bar{u}_1}{\partial\bar{x}}+\bar{u}_1\frac{\partial\bar{u}_0}{\partial\bar{x}}+\bar{v}_1\frac{\partial\bar{u}_1}{\partial\bar{Y}}+\bar{v}_2\frac{\partial\bar{u}_0}{\partial\bar{Y}}=\frac{\partial^2\bar{u}_1}{\partial\bar{Y}^2}+5\bar{\theta}_1 \quad (13b)$$

$$\frac{\partial\bar{p}_1}{\partial\bar{Y}}=0 \quad (13c)$$

$$\bar{u}_0\frac{\partial\bar{w}_1}{\partial\bar{x}}+\bar{v}_1\frac{\partial\bar{w}_1}{\partial\bar{Y}}=\frac{\partial^2\bar{w}_1}{\partial\bar{Y}^2} \quad (13d)$$

$$\bar{u}_0\frac{\partial\bar{\theta}_1}{\partial\bar{x}}+\bar{u}_1\frac{\partial\bar{\theta}_0}{\partial\bar{x}}+\bar{v}_1\frac{\partial\bar{\theta}_1}{\partial\bar{Y}}+\bar{v}_2\frac{\partial\bar{\theta}_0}{\partial\bar{Y}}=\frac{1}{Pr}\frac{\partial^2\bar{\theta}_1}{\partial\bar{Y}^2}. \quad (13e)$$

The $\bar{w}_1$ distribution is determined directly from equation (13d) using the asymptotic result (12c). The appropriate boundary conditions for $\bar{w}_1$ are

$$\bar{w}_1=0 \quad \text{at } \bar{Y}=0,$$

$$\bar{w}_1\to W_1(x,0,z) \quad \text{as } \bar{Y}\to\infty.$$

It is assumed that

$$\bar{w}_1\sim\gamma\bar{x}^{-1/5}H_0'(\eta).$$

With $\bar{u}_0$ and $\bar{v}_1$ given by equations (8), the equation governing $H_0'(\eta)$ becomes

$$H_0'''(\eta)+4f_0(\eta)H_0''(\eta)+f_0'(\eta)H_0'(\eta)=0$$

$$H_0'(0)=0, \quad H_0'(\infty)=1. \quad (14)$$

The solutions for $\bar{u}_1$, $\bar{v}_2$ and $\bar{\theta}_1$ can be obtained in a similar manner. If we write

$$\bar{u}_1=-\frac{5}{2}\gamma\bar{x}^{-1/5}f_1'(\eta)$$

$$\bar{v}_2=-\frac{\gamma}{2}\bar{x}^{-1}\eta f_1'(\eta)$$

$$\bar{\theta}_1=-\frac{\gamma}{2}\bar{x}^{-3/5}t_1(\eta) \quad (15)$$

then we easily find that $f_1(\eta)$ and $t_1(\eta)$ satisfy the following equations:

$$f_1'''+4f_0f_1''-2f_0'f_1'+t_1=0$$

$$\frac{1}{Pr}t_1''+4f_0t_1'+3f_0't_1-t_0f_1'=0$$

$$f_1(0)=f_1'(0)=t_1(\infty)=t_1'(0)=0$$

$$f_1'(\infty)=\frac{4}{5}\gamma\cot\frac{\pi}{5}. \quad (16)$$

Equations (16) are the same as those governing the second-order boundary layer flows for a two-dimensional vertical flat plate [3].

The far-field boundary conditions for the flow in the corner layer are described finally as follows:

$$u\sim 5f_0'(\eta), \quad v\sim\eta f_0'(\eta)-4f_0(\eta), \quad w\sim\gamma H_0'(\eta)$$

$$\omega\sim\gamma H_0''(\eta), \quad \theta\sim t_0(\eta). \quad (17)$$

Considering symmetry properties (4), we have the asymptotic conditions as $\eta\to\infty$, $\zeta/\eta\to 0$

$$u\sim 5f_0'(\zeta), \quad v\sim\gamma H_0'(\zeta), \quad w\sim\zeta f_0'(\zeta)-4f_0'(\zeta)$$

$$\omega\sim-\gamma H_0''(\zeta), \quad \theta\sim t_0(\zeta). \quad (18)$$

The corner-layer equations (3) with boundary conditions (5), (17) and (18) can be rewritten in a more convenient form by introducing 'the velocity potentials' ϕ and φ, and 'the modified vorticity' Ω, defined as follows:

$$\phi=\frac{\eta u}{5}-v, \quad \varphi=\frac{\zeta u}{5}-w$$

$$\Omega=\varphi_\eta-\phi_\zeta. \quad (19)$$

The resulting corner-layer equations are

$$\nabla^2u+\phi u_\eta+\varphi u_\zeta-\frac{3}{5}u^2+5\theta=0$$

$$\nabla^2\Omega+\phi\Omega_\eta+\varphi\Omega_\zeta+u\left[\Omega+\frac{8}{25}(\eta u_\zeta-\zeta u_\eta)\right]+\zeta\theta_\eta-\eta\theta_\zeta=0$$

$$\nabla^2\phi+\Omega_\zeta-u_\eta=0$$

$$\nabla^2\varphi-\Omega_\eta-u_\zeta=0$$

$$\frac{1}{Pr}\nabla^2\theta+\phi\theta_\eta+\varphi\theta_\zeta-\frac{u}{5}\theta=0 \quad (20)$$

and the boundary conditions are written as

$$u=\phi=\varphi=0, \quad \Omega=\varphi_\eta, \quad \theta_\eta=-1 \quad \text{at } \eta=0;$$

$$u=\phi=\varphi=0, \quad \Omega=-\phi_\zeta, \quad \theta_\zeta=-1 \quad \text{at } \zeta=0;$$

$$u\sim 5f_0'(\eta), \quad \Omega\sim\zeta f_0''(\eta)-\gamma H_0''(\eta), \quad \phi\sim 4f_0(\eta)$$

$$\varphi\sim\zeta f_0'(\eta)-\gamma H_0'(\eta), \quad \theta\sim t_0(\eta) \quad \text{as } \zeta\to\infty, \quad \eta/\zeta\to 0;$$

$$u\sim 5f_0'(\zeta), \quad \Omega\sim-\eta f_0''(\zeta)+\gamma H_0''(\zeta), \quad \phi\sim\eta f_0'(\zeta)-\gamma H_0'(\zeta)$$

$$\varphi\sim 4f_0(\zeta), \quad \theta\sim t_0(\zeta) \quad \text{as } \eta\to\infty, \quad \zeta/\eta\to 0. \quad (21)$$

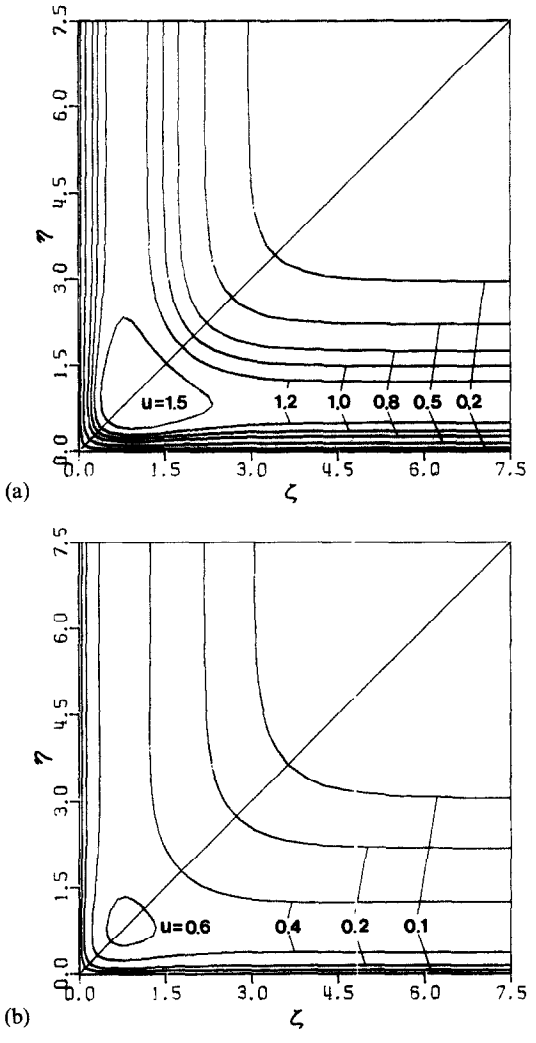

FIG. 2. Streamwise isovels: (a) $Pr = 0.733$; (b) $Pr = 6.7$.

3. METHOD OF SOLUTION

Corner-layer equations (20) and boundary conditions (21) are similar to those of ref. [10], and the procedure for numerical solutions is closely paralleled: we introduce new variables $\bar{\phi}$, $\bar{\Omega}$ and $\bar{\varphi}$ instead of ϕ, Ω and φ

$$\bar{\phi} = \phi - \eta f'_0(\zeta)$$
$$\bar{\Omega} = \Omega - \eta f''_0(\zeta) - \zeta f''_0(\eta)$$
$$\bar{\varphi} = \varphi - \zeta f'_0(\eta) \tag{22}$$

and then transform the unbounded region $0 \leqslant \eta, \zeta \leqslant \infty$ into a finite computational domain $0 \leqslant N, S \leqslant 1$ by

$$N = \frac{a\eta}{1+a\eta}, \quad S = \frac{a\zeta}{1+a\zeta} \tag{23}$$

where a is a grid-spacing parameter. A uniform grid in the computational plane gives a non-uniform grid in the physical plane with the grids being more heavily concentrated near the corner.

The corner-layer equations and the boundary conditions rewritten in terms of the new defined variables are solved numerically by the alternate direction implicit scheme used in ref. [10]. The mesh size H and the grid-spacing parameter a that were used earlier [10] are also found adequate in the present analysis

$$H = 0.02, \quad z = 0.2.$$

The solution is considered to have converged when the variation in successive iterations becomes less than 10^{-4} as done in ref. [10].

4. RESULTS AND DISCUSSION

The numerical results for $Pr = 0.733$ and 6.7 are presented in Figs. 2–5. Figure 2 shows streamwise isovels. The distributions of streamwise velocity u are

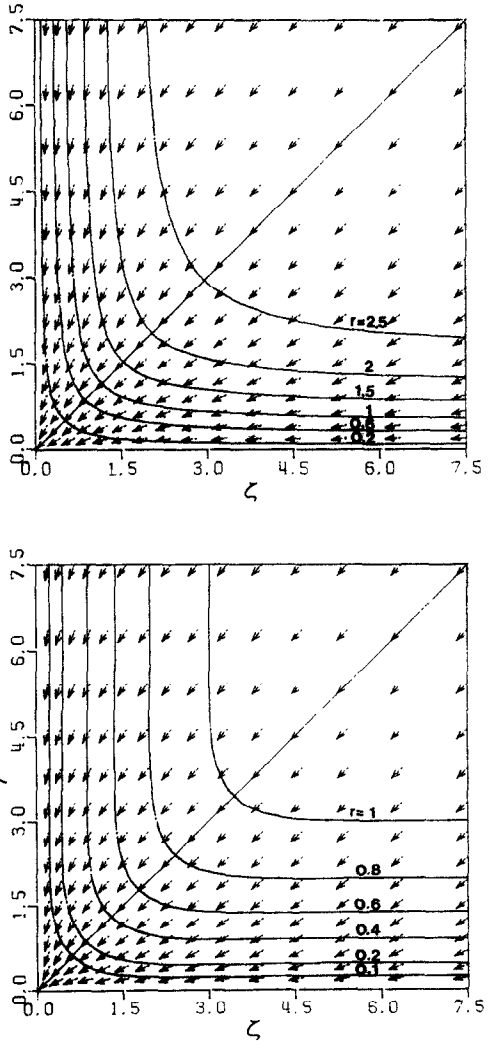

FIG. 3. Magnitudes and directions of crossflow: (a) $Pr = 0.733$; (b) $Pr = 6.7$.

similar to those for the isothermal surfaces: closed contours of u due to the mutual interaction of the boundary layers appear in the vicinity of the symmetry plane near the corner. The thickness of the velocity boundary layer has its maximum value at the symmetry plane and decreases monotonically to its asymptotic two-dimensional value as $\zeta \to \infty$.

Isolines of $r = (v^2+w^2)^{1/2}$, the magnitude of the crossflow, and the directions $\Theta = \tan^{-1}(v/w)$ are depicted in Fig. 3. The crossflow converges almost radially towards the corner. This converging flow increases the amount of flow entrainment near the corner and, therefore, the streamwise velocity exhibits the distributions discussed above. As seen in Figs. 2 and 3, the magnitude of velocity decreases and the thickness of velocity boundary layer increases with Prandtl number.

The dimensionless temperature distributions are shown in Fig. 4. It is observed that the temperature profiles are similar to those for the isothermal corner except in the interior region near the corner. Figure 5 illustrates the local Nusselt number Nu, which is inversely proportional to the surface temperature $\theta(0, \zeta)$

$$Nu = \frac{1}{\theta(0,\zeta)}\left(\frac{Gr^*}{5}\right)^{1/5}. \tag{24}$$

The surface temperature (the local Nusselt number) has a maximum (minimum) value at the corner and decreases (increases) monotonically to an asymptotic value corresponding to the two-dimensional problem. The results are consistent with those of ref. [10]. The isothermal results [10] reveal that the local heat transfer rate changes appreciably near the corner and becomes essentially constant at a distance (larger for smaller Prandtl number) from the vertex. Thus, the temperature profiles for isoflux walls differ from those for isothermal walls only in a close neighbourhood of the corner, and become similar as the distance from the corner increases. The region which shows different temperature profiles is wider for smaller Prandtl number.

Figure 5 also illustrates the distributions of wall shear stress which is given by, neglecting the effects of the crossflow

$$\tau_w = \frac{\tau_{w\infty}}{f_0''(0)} u_\eta(0,\zeta) \tag{25}$$

where

$$\tau_{w\infty} = \frac{\rho v^2}{x^2} f_0''(0)\left(\frac{Gr^*}{5}\right)^{3/5}.$$

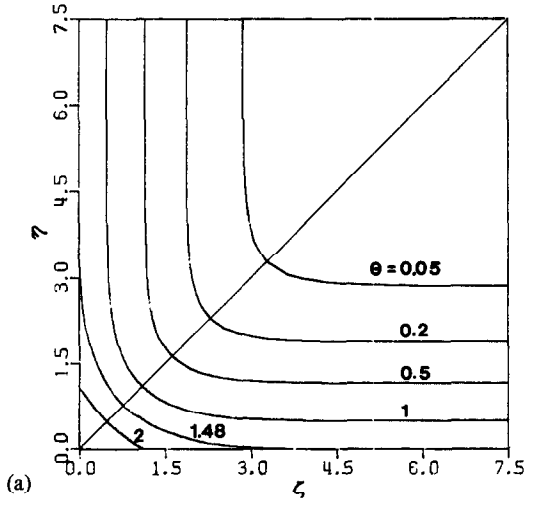

(a)

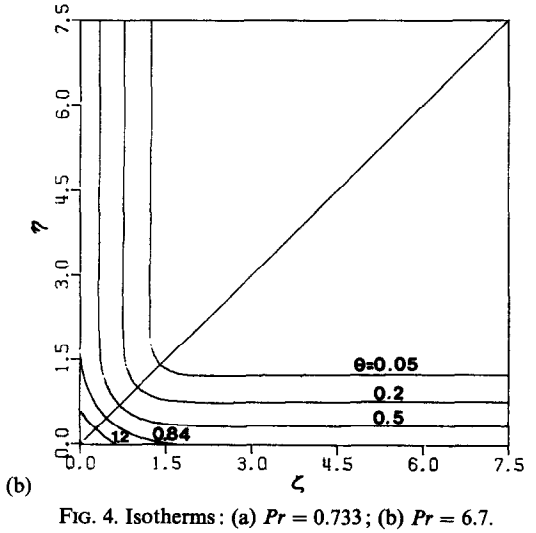

(b)

FIG. 4. Isotherms: (a) $Pr = 0.733$; (b) $Pr = 6.7$.

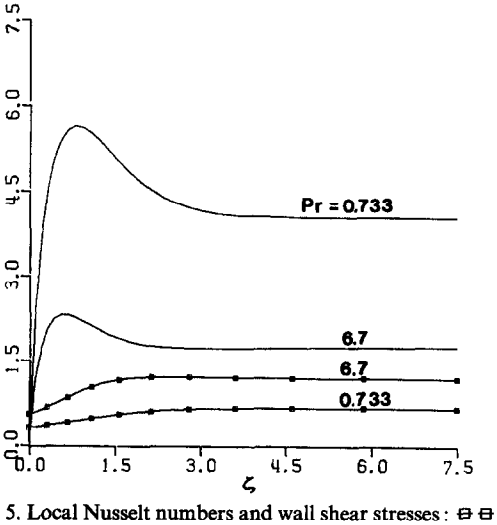

FIG. 5. Local Nusselt numbers and wall shear stresses: ⊟ ⊟, $Nu(0,\zeta)(Gr^*/5)^{-1/5}$; ——, $\tau_w(0,\zeta)(f''(0)/\tau_{w\infty})$.

The general trend for local shear stress distributions is similar to that for the isothermal case: τ_w is zero at the corner and attains its maximum at a certain distance from the vertex and then tends to its asymptotic two-dimensional value. As compared with the isothermal walls, the magnitude of overshoot is larger for the isoflux case. This can be expected physically since the variation of temperature distributions near the corner is greater for isoflux walls and the buoyancy force becomes more pronounced.

REFERENCES

1. K. T. Yang and E. W. Jerger, First order perturbations of laminar free-convection boundary layers on a vertical plate, *J. Heat Transfer* **86,** 107–115 (1964).
2. C. A. Hieber, Natural convection around a semi-infinite vertical plate: higher order effects, *Int. J. Heat Mass Transfer* **17,** 785–795 (1974).
3. R. L. Mahajan and B. Gebhart, Higher order approximations to the natural convection flow over a uniform flux vertical surface, *Int. J. Heat Mass Transfer* **21,** 549–556 (1978).
4. K. Stewartson, On the free convection from horizontal plates, *Z. Angew. Math. Phys.* **9,** 276–282 (1958).
5. L. Pera and B. Gebhart, Natural convection boundary layer flow over horizontal and slightly inclined surfaces, *Int. J. Heat Mass Transfer* **16,** 1131–1146 (1973).
6. T. S. Chen, H. C. Tien and B. F. Armaly, Natural convection on horizontal, inclined and vertical plates with variable surface temperature or heat flux, *Int. J. Heat Mass Transfer* **29,** 1465–1478 (1986).
7. D. B. Ingham, Transient free convection on an isothermal vertical flat plate, *Int. J. Heat Mass Transfer* **21,** 67–69 (1978).
8. P. Luichini, Analytical and numerical solutions for natural convection in a corner, *AIAA J.* **24,** 841–848 (1986).
9. C. Y. Liu and A. C. Guerra, Free convection in a porous medium near the corner of arbitrary angle formed by two vertical plates, *Int. Commun. Heat Mass Transfer* **12,** 431–440 (1985).
10. M. H. Kim and M.-U. Kim, Natural convection near a rectangular corner, *Int. J. Heat Mass Transfer* **31,** 1357–1364 (1988).
11. S. G. Rubin, Incompressible flow along a corner, *J. Fluid Mech.* **26,** 97–110 (1966).

CONVECTION NATURELLE PRES D'UN DIEDRE DROIT FORME PAR DEUX PLANS VERTICAUX AVEC DENSITE DE FLUX THERMIQUE UNIFORME

Résumé—On considère la convection naturelle laminaire le long d'un angle rectangle formé par l'intersection de deux plans verticaux infinis avec densité de flux thermique uniforme sur les surfaces. Pour des grands nombres de Grashof, les équations de couche limite au bord d'attaque qui gouvernent le comportement de la convection naturelle laminaire près du coin sont établies et les conditions aux limites appropriées sont déterminées en utilisant la méthode des développements asymptotiques. Les solutions des équations sont obtenues numériquement pour des nombres de Prandtl de 0,733 et 6,7. Les configurations générales de l'écoulement et des distributions de température sont semblables à celles relatives à des conditions de température uniforme à l'exception des profils de température près du coin.

NATÜRLICHE KONVEKTION IN DER NÄHE EINER ECKE, DIE VON ZWEI RECHTWINKLIG ANGEORDNETEN UND MIT KONSTANTER WÄRMESTROMDICHTE BEHEIZTEN SENKRECHTEN PLATTEN GEBILDET WIRD

Zusammenfassung—Es wird die laminare natürliche Konvektionsströmung entlang einer Ecke, die durch den rechtwinkligen Schnitt zweier viertelunendlicher senkrechter Platten gebildet wird, betrachtet. Die bestimmenden Gleichungen für die Grenzschicht in der Ecke, die das Verhalten der laminaren Strömung durch natürliche Konvektion beschreiben, werden für große Werte der Grashof-Zahl hergeleitet. Die geeigneten Randbedingungen werden mit der Methode der angepaßten asymptotischen Näherung gewonnen. Die Gleichungen werden numerisch für die Prandtl-Zahlen 0,733 und 6,7 gelöst. Die Strömungsbilder und Temperaturverteilungen gleichen im wesentlichen denen, die man im Falle konstanter Wandtemperaturen erhält, mit Ausnahme der Temperaturverteilung in der Ecke.

ЕСТЕСТВЕННАЯ КОНВЕКЦИЯ ВБЛИЗИ ПРЯМОГО УГЛА, ОБРАЗОВАННОГО ДВУМЯ ВЕРТИКАЛЬНЫМИ ПЛОСКИМИ ПЛАСТИНАМИ С РАВНОМЕРНЫМ ТЕПЛОВЫМ ТЕПЛОВЫМ ПОТОКОМ НА ПОВЕРХНОСТИ

Аннотация—Исследуется ламинарное естественноконвективное течение у прямого угла, образованного пересечением двух вертикальных полуограниченных плоских пластин с равномерным тепловым потоком на поверхности. Для больших чисел Грасгофа с точностью до главных членов получены уравнения, описывающие течение вблизи угловой зоны, определяющие характер ламинарного естественноконвективного течения, а также определены соответствующие граничные условия методом сращиваемых асимптотических разложений. Получены численно решения этих уравнений для чисел Прандтля, изменяющихся от 0,733 до 6,7. Общая структура течения и распределение температуры подобны полученным для равномерной температуры стенок, за исключением температурных профилей вблизи угла.